



## Behaviour of molybdate-passivated zinc coated steel exposed to corrosive chloride environments

G. M. TREACY\*, G. D. WILCOX and M. O. W. RICHARDSON  
IPTME, Loughborough University, Loughborough, Leicester, LE11 3TU, Great Britain  
(\*author for correspondence, e-mail: g.treacy@lboro.ac.uk)

Received 13 March 1998; accepted in revised form 17 November 1998

*Key words:* conversion coatings, corrosion, impedance, molybdate, passivation

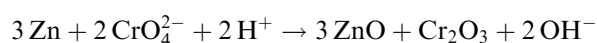
### Abstract

The behaviour of molybdate conversion coatings on zinc coated mild steel in corrosive chloride environments was investigated using electrochemical impedance spectroscopy (EIS), X-ray photoelectron spectroscopy (XPS) and neutral salt fog exposure. It was found that the presence of a simple molybdate coating initially increased the rate of corrosion of zinc. Molybdenum species were initially present in the conversion coating in either the +V or +VI oxidation states. Exposure to neutral salt fog reduced molybdenum to either Mo(IV) or Mo(III). This reduction of molybdenum, an additional cathodic process, may result in the activation of zinc observed in these studies. For molybdate-passivated surfaces in the early stages of exposure to neutral salt fog, corrosion products were found to be less voluminous than those observed on untreated surfaces. This may be due to the presence of inhibiting Mo(IV) or Mo(III) species in the corrosion product layers. However, after 24 h exposure to salt fog, no molybdenum could be detected. This implies that the lower oxidation state molybdenum species formed are soluble. However, surfaces passivated from molybdate solutions appear to forestall the onset of red rust, during immersion in chloride solutions and exposure to salt fog, by approximately 12 to 24 h. This behaviour may be attributable to corrosion inhibition by Mo(III) and Mo(IV) species while they are present at the surface.

### 1. Introduction

There is much evidence that molybdate species possess good corrosion inhibition properties [1–3]. They are also oxyanion analogues of chromate. As a result they have been widely considered as possible alternatives to chromate for the corrosion protection of zinc substrates [4–9]. In addition, molybdate-based conversion coatings are attractive alternatives to chromate due to their relatively low toxicity [4].

It has been proposed that the efficacy of chromate conversion coatings, with respect to the provision of corrosion resistance, is attributable to the ability of such coatings to act as effective barriers and to repair themselves at sites of coating damage due to the presence of a 'reservoir' of Cr(VI) [10]. Passivation of zinc surfaces by chromate solutions is ascribed to the formation of mixed oxides, probably in the form of a spinel structure, according to the following reaction [11, 12]:



Evidence exists that molybdenum is present in both the (IV) and (V) oxidation states in films formed on zinc substrates [13]. It might be thought that the presence of a reservoir of Mo(VI) would allow such coatings to self-repair in a similar manner to that observed in chromate coatings. However, there is little evidence that molybdate coatings possess such a capability. This may be due to the fact that molybdate is a weaker oxidising agent than chromate. However, it does appear that the presence of molybdate conversion coatings on zinc-based substrates does improve the corrosion resistance of the substrate, but to a lesser extent than chromate-based coatings [14]. However, in combination with another coating agents, such as phosphoric acid, good corrosion resistance has been reported, especially during outdoor exposure trials [9]. It has been noted that these treatments perform, in certain circumstances, less well under neutral salt spray conditions and require an sealant layer to attain corrosion resistance similar to that provided by chromate-based coatings.

In these studies the behaviour of simple molybdate coatings on zinc-plated mild steel in a corrosive chloride environment was investigated using electrochemical impedance spectroscopy (EIS). Analysis of the elemental composition of the surface layers was also carried out using x-ray photoelectron spectroscopy (XPS). Using these data it was hoped that the mechanism of interaction between the zinc substrate and the molybdate coating could be identified.

## 2. Experimental details

A coating of nominally  $8\ \mu\text{m}$  of zinc was electrodeposited onto mild steel coupons,  $25\ \text{cm}^2$  in area, from a proprietary alkaline noncyanide bath. Molybdate conversion coatings were formed on these surfaces by immersion in  $0.1\ \text{mol dm}^{-3}\ \text{Na}_2\text{MoO}_4 \cdot 2\ \text{H}_2\text{O}$ , adjusted to pH 5.0 with  $\text{HNO}_3$ , for 5 min at room temperature producing a typically iridescent finish [14]. These panels were then immersed in 3.5% NaCl and their corrosion resistance was evaluated using electrochemical impedance spectroscopy (EIS). Measurements were taken using an EG&G Parc potentiostat/galvanostat (model 263A), coupled to an EG&G 5210 two-phase lock-in amplifier. The instruments were controlled via EG&G Parc (model 398) impedance software. The impedance spectra were collected at open circuit potential (OCP), with a 5 mV amplitude, using a standard calomel electrode as reference and platinum sheet as an auxiliary electrode. Data were collected between 5 kHz and 100 mHz. The results were mathematically modelled using EQUIVCRT by Boukamp [15].

Surface analysis of uncorroded and corroded samples, using X-ray photoelectron spectroscopy (XPS), was also carried out. Molybdate passivated zinc coupons were placed in a CW Specialist Equipment Ltd (model SF4 500 CASS) salt fog cabinet operating according to ASTM B117. These samples were removed at 3, 7 and 24 h salt fog exposure. Elemental analysis was carried out on a VG Escalab (mark 1) instrument using aluminium  $K_{\alpha}$  X-rays of 1486.6 eV in energy.

The behaviour of molybdate-passivated surfaces over prolonged exposure to salt spray was also evaluated using ASTM B117. Tests were carried out, in duplicate, on mild steel panels,  $150\ \text{cm}^2$  in area, with nominally  $8\ \mu\text{m}$  of zinc electrodeposited from the proprietary bath. A molybdate conversion coating was then formed on these panels using the same conditions described above. A batch of untreated zinc electrodeposited steel panels were also tested for reference. Time taken for the appearance of zinc corrosion products (white rust) and iron corrosion products (red rust) were noted.

## 3. Results and discussion

In Figure 1(a) experimental electrochemical impedance data for molybdate-passivated zinc electrodeposited mild steel, immersed in 3.5% NaCl over 168 h, is presented in the Nyquist format. It is evident that two merged semicircles exist on the spectra, with Warburg impedance becoming more apparent with increasing immersion time. The semicircles can be attributed to the separate responses of the conversion coating and the underlying substrate. This is confirmed by the presence of only a single semicircle, with Warburg impedance, observed for uncoated zinc electrodeposited mild steel in 3.5% NaCl (Fig. 2). It is known that the morphology of molybdate coatings on zinc coated steel surfaces resemble a 'dry river bed' [14]. This suggests that these coatings are cracked and may allow corrosive ions access to the substrate metal. Therefore, it appears that these coatings act as weak barriers to corrosion. Warburg impedance, due to diffusion control of surface

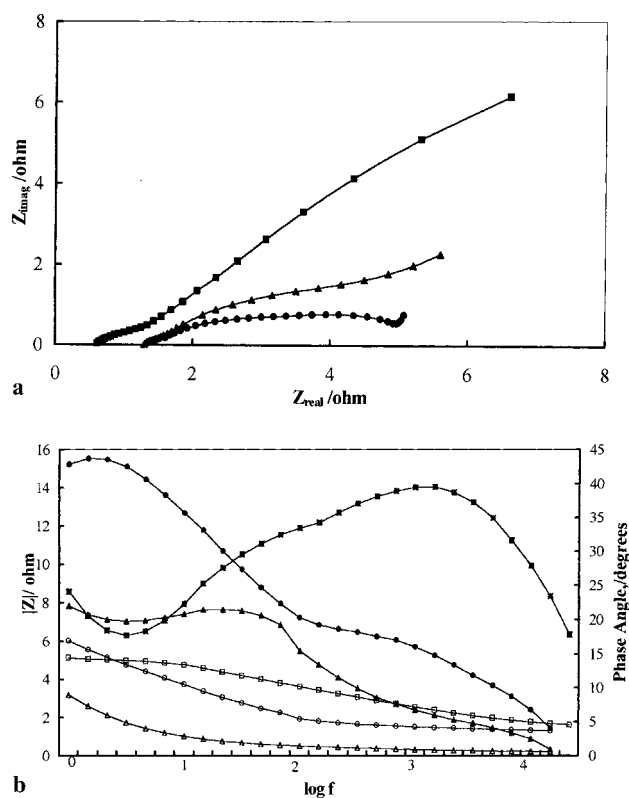


Fig. 1. (a) Impedance data for molybdate treated zinc electrodeposited mild steel immersed for: (●) 0 h, (▲) 24 h and (■) 168 h in 3.5% NaCl over 168 h in complex plane format. (b) Impedance data for molybdate treated zinc electrodeposited mild steel immersed in 3.5% NaCl over 168 h in Bode format. Key: (□) Bode impedance 0 h; (■) Bode phase 0 h; (○) Bode impedance 24 h; (●) Bode phase 24 h; (▽) Bode impedance 168 h; (▲) Bode phase 168 h.

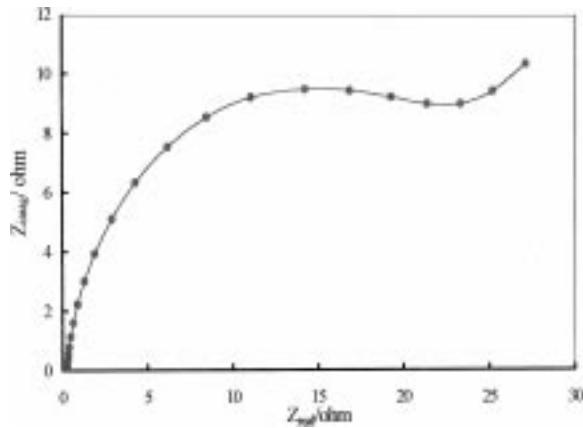


Fig. 2. Nyquist impedance data for untreated zinc electrodeposited mild steel immersed in 3.5% NaCl.

processes, resulting from the oxidation of zinc and the quiescent nature of the electrolyte, is evident in the low frequency region (Fig. 1(a)).

In Figure 1(b) the same experimental data is displayed in the Bode format. It can be seen that the modulus of impedance ( $|Z|$ ) increases slightly at low frequencies after 24 h and then decreases once more. However, overall  $|Z|$  tends to decrease with increasing immersion time. The maximum phase angle is displaced towards lower frequencies with increasing immersion time. After 24 h immersion in 3.5% NaCl white rust was evident over much of the sample surface. It is felt that the general decrease in  $|Z|$  within 24 h immersion is indicative of an increase in corrosion rate of the passivated surface. The onset of diffusion control of surface processes, as a result of the build up of white rust on the metal surface, is also evident after 24 h immersion with the increase in  $|Z|$  at low frequencies (Figure 1(b)). The shift of maximum phase angle towards lower frequencies may also be attributable to zinc oxidation resulting in the formation of white rust on the metal surface.

Using Boukamp's EQUIVCRT [15], mathematical modelling of the experimental results was carried out. In the initial stages of immersion the equivalent circuit shown in Figure 3(a) was used, while that displayed in Figure 3(b) was employed for immersion times of 24 h and above. The values of the equivalent circuit components for molybdate treated surfaces, estimated by EQUIVCRT, are presented in Table 1. These equivalent circuits were found to fit the experimental data quite well, as can be seen from the comparison of experimental and simulated data for molybdate treated zinc coated steel immersed in 3.5% NaCl for 24 h produced by EQUIVCRT presented in Figure 4. The constant phase element (CPE)  $Q_1$  can be attributed to the capacitance of

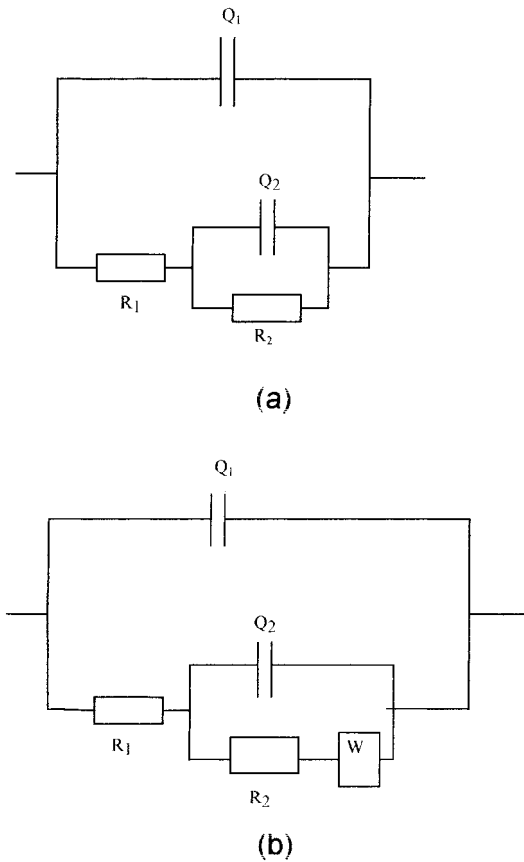


Fig. 3. Equivalent circuit for molybdate treated zinc electrodeposited mild steel immersed in 3.5% NaCl (a) uncorroded and (b) after the onset of corrosion.

the film present on the surface (Figs 3(a) and (b) and Table 1). Initially this is due to the conversion layer, but with time can be attributed to the film of white rust present at the surface. This value is relatively large, due to the quiescent nature of the electrolyte and the electrode activity. The CPE  $Q_2$  can be attributed to the capacitance of the double layer. The conversion layer resistance,  $R_1$ , after an initial decrease remained quite constant and consistently small, indicating that these coatings act only as weak barriers. The charge transfer resistance,  $R_2$ , was also relatively consistent until 168 h immersion. There was a slight increase in  $R_1$  after 72 h exposure perhaps due to the slightly protective nature of the white rust present on these surfaces. In the latter stages of neutral salt fog exposure  $R_2$  values decreased due to the development of red rust (Table 1).

In Table 2 the results of mathematical modelling, using EQUIVCRT, of the impedance data obtained for untreated zinc electrodeposited steel immersed in 3.5% NaCl over 196 h are presented. Initially the equivalent circuit used to model these data was a simple Randles

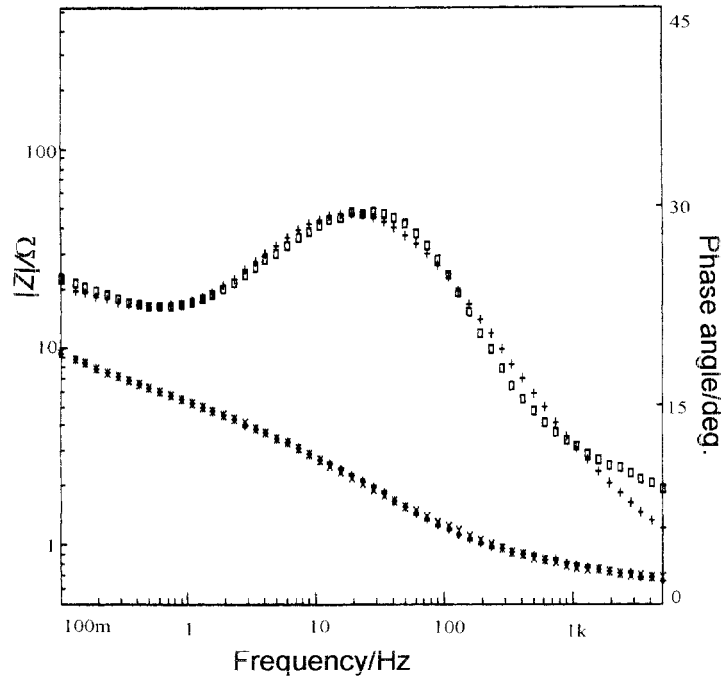


Fig. 4. Fit of the equivalent circuit from Figure 3(b) to experimental data for molybdate treated zinc coated steel after 24 h immersion in 3.5% NaCl, using Boukamp's EQUIVCRT. Key: (◆) measured Bode impedance, (×) simulated Bode impedance, (□) measured Bode phase angle, (+) simulated Bode phase angle.

Table 1. Impedance data obtained from Boukamp analysis of experimental impedance results of molybdate conversion treatments on zinc electrodeposited mild steel immersed in 3.5% NaCl

Immersion time/h	$Q_1/F$	$R_1/\Omega$	$R_2/\Omega$	$Q_2/F$	$W/\Omega s^{-1}$
0	$3.76 \times 10^{-5}$	0.4486	3.913	$2.43 \times 10^{-2}$	–
24	$2.03 \times 10^{-4}$	0.2804	3.068	$1.13 \times 10^{-2}$	$1.41 \times 10^{-1}$
48	$7.57 \times 10^{-3}$	0.2334	2.076	$8.51 \times 10^{-3}$	$1.33 \times 10^{-1}$
72	$1.36 \times 10^{-4}$	0.2857	5.851	$1.64 \times 10^{-2}$	$1.63 \times 10^{-1}$
168	$2.34 \times 10^{-4}$	0.4203	0.518	$1.27 \times 10^{-2}$	$3.31 \times 10^{-2}$
192	$1.21 \times 10^{-4}$	0.3464	1.086	$5.42 \times 10^{-3}$	$3.91 \times 10^{-2}$

cell with Warburg impedance (Fig. 5) as the metallic surface was uncorroded. However, as white rust built up on the panel surface the equivalent circuit displayed in Figure 3(b) became more appropriate due to the presence of corrosion layers. From Table 2 it can be seen that as white rust builds up on these panels that a value for  $R_1$ , a layer resistance, is recorded, due to the presence of the corrosion layer. This value remains relatively constant throughout the remainder of the experiment.  $R_2$ , the charge transfer resistance, increases due to the build up of white rust on these surfaces, which provides the surface with a small degree of corrosion protection

Table 2. Representative impedance data obtained from modelling of experimental results by Boukamp for untreated zinc electrodeposited mild steel immersed in 3.5% NaCl

Immersion time/h	$Q_1/F$	$R_1/\Omega$	$R_2/\Omega$	$Q_2/F$	$W/\Omega s^{-1}$
0	–	–	17.09	$5.15 \times 10^{-4}$	$2.68 \times 10^{-2}$
24	–	–	2.38	$1.42 \times 10^{-2}$	$1.45 \times 10^{-1}$
47	$3.69 \times 10^{-4}$	0.5632	2.76	$2.92 \times 10^{-2}$	$1.50 \times 10^{-1}$
76	$1.36 \times 10^{-3}$	0.2522	5.67	$2.05 \times 10^{-2}$	$1.60 \times 10^{-1}$
98	$4.38 \times 10^{-4}$	0.2858	10.07	$3.80 \times 10^{-2}$	$4.01 \times 10^{-1}$
116	$6.88 \times 10^{-4}$	0.5269	16.13	$4.22 \times 10^{-2}$	–
149	$3.06 \times 10^{-3}$	0.2014	11.84	$2.00 \times 10^{-2}$	$9.04 \times 10^{-2}$
166	$3.04 \times 10^{-3}$	0.1874	2.52	$1.54 \times 10^{-2}$	$2.58 \times 10^{-2}$
196	$3.14 \times 10^{-2}$	0.2677	0.72	$4.99 \times 10^{-3}$	$7.04 \times 10^{-2}$

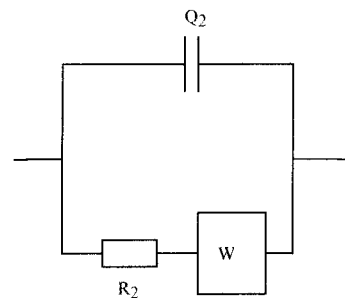


Fig. 5. Equivalent circuit for uncorroded untreated zinc electrodeposited mild steel panels.

as surface processes come increasingly under diffusion control. This is evidenced by the presence of Warburg diffusion (Table 2, Fig. 2). After 116 h exposure no Warburg diffusion could be detected on the impedance spectra. This was unexpected and cannot be adequately explained, however, as immersion time increased further Warburg was once again discerned.

Comparing these data (Table 2) with those obtained for molybdate treated zinc electrodeposited steel panels (Table 1) it can be seen that the presence of the molybdate coating has a profound effect on the impedance response of the zinc electrodeposited surface. This can be seen more clearly in Figure 6 where a graph of  $R_{tot} = R_1 + R_2$  against immersion time in 3.5% NaCl, for both molybdate-coated and uncoated zinc electrodeposited mild steel, is presented. It can be seen that  $R_{tot}$  remains relatively stable for molybdate coated zinc surfaces up to 168 h immersion. For the uncoated surface the initial  $R_{tot}$  value is much higher than that obtained for molybdate-coated zinc, implying that the presence of the conversion coating has increased the rate of corrosion of these zinc surfaces.

After 24 h immersion,  $R_{tot}$  values for unpassivated zinc drop to the same levels as those observed for molybdate-coated zinc, due to the formation of insol-

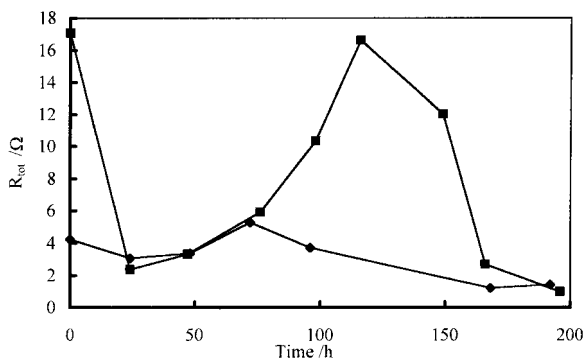


Fig. 6. Graph of the variation of  $R_{tot}$  with immersion time for (■) untreated and (◆) molybdate treated zinc electrodeposited surfaces immersed in quiescent 3.5% NaCl.

uble corrosion products. However, a further increase is observed after 76 h immersion due to the somewhat protective nature of the white corrosion film. This may be due to its rather voluminous nature causing an increase in diffusion control. This behaviour is not observed for molybdate passivated panels. Despite this apparent activation of the metal surface by the molybdate coating, red rust was not observed on these surfaces until 12 to 24 h after its appearance on unpassivated samples during immersion in 3.5% NaCl. Further evidence exists that the presence of molybdate-based coatings extends the time before the first signs of red rust were observed during salt fog exposure, according to ASTM B117 (Table 3). This extension of time taken before iron corrosion products, in the form of red rust, were noted by other authors [9, 14].

Investigations into alterations in the chemical state and concentration of molybdenum present at the metal surface were carried out using XPS. Both uncorroded and corroded samples, which had been exposed to salt fog for 3, 7 and 24 h, were examined. The elemental composition at these surfaces are presented in Table 4, while in Figure 7 a broad scan XPS spectrum, obtained for molybdate passivated zinc electrodeposited mild steel exposed to salt spray for 3 h, is displayed. It is evident that no chlorine was detected at the surface for uncorroded molybdate passivated samples (Table 4). However, after just 3 h salt fog exposure high levels of chlorine, too high to be solely attributed to a sodium chloride residue, were found. The specimens were thoroughly washed before analysis and no sodium was detected at the surface, implying that chlorine had become incorporated into the surface layers during corrosion. A proportion of this would be expected to be associated with zinc hydroxychloride complexes formed due to zinc corrosion in a chloride rich environment [16]. It was observed that the concentration of zinc at the surface increased after 3 h exposure to salt fog and then remained fairly constant up to 24 h exposure. It is also evident that after 24 h exposure to salt spray no molybdenum could be detected at the metal surface. In

Table 3. Neutral salt spray corrosion resistance data, according to ASTM B117, for zinc electrodeposited mild steel substrates, untreated and with a molybdate conversion coating

Sample	Appearance						
	0 h	21 h	45 h	66 h	90 h	150 h	177 h
MoO <sub>4</sub> <sup>2-</sup> , pH 5	uncorroded	small amount of white rust	white rust has increased	further increase in white rust	small amount of red rust	red rust	red rust
Uncoated	uncorroded	more severe white rust	more severe than molybdate-passivated panels	extensive white rust	extensive red rust	red rust	red rust

Table 4. XPS Data for molybdate treated zinc electrodeposited mild steel panels exposed to salt fog

Sample	Surface composition/at %				
	C	O	Cl	Mo	Zn
Unexposed	23.8	49.9	—	20.9	5.3
3 h exposure	38.7	42.3	5.7	1.1	12.2
7 h exposure	34.7	47.4	3.9	0.7	13.2
24 h exposure	35.0	48.8	3.6	—	12.6

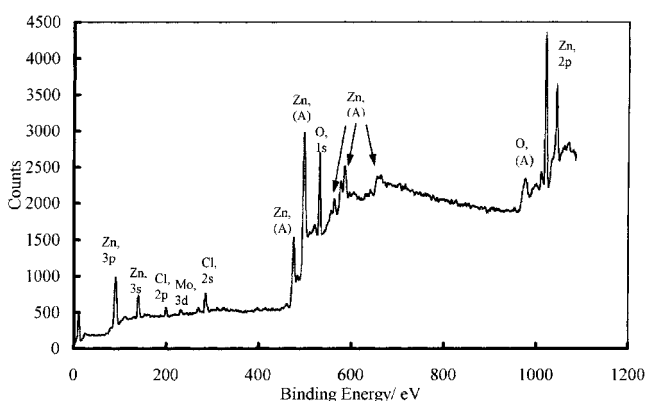


Fig. 7. XPS spectrum for molybdate treated zinc electrodeposited mild steel exposed to salt spray for 3 h. (A: Auger peaks)

addition, the concentration of chlorine decreased with increasing exposure time. This indicates that some chlorine may be associated with molybdenum at the metal surface and is being lost with these species with increasing salt fog exposure time.

Determination of the chemical state of molybdenum at these surfaces, using high resolution XPS, showed that, on uncorroded panels, molybdenum had a binding energy of 231.5 eV. This indicates that it is present in the uncorroded conversion coating in a high oxidation state; either (V), (VI) or, possibly, a mixture of the two. After 3 and 7 h exposure to salt fog the binding energy of molybdenum species at the surface had shifted to 230.3 and 230.6 eV, respectively. This implies that molybdenum had been reduced during the formation of corrosion products. This shift in the binding energy of molybdenum between uncorroded and corroded molybdate passivated surfaces can be more clearly seen in Figure 8(a) and (b) where the XPS peaks assigned to Mo 3d, for uncorroded and corroded molybdate passivated zinc electrodeposited steel surfaces, are presented. A binding energy in the region of 230.6 eV, obtained for molybdenum on passivated samples exposed to salt fog for 3 and 7 h, indicates that it could be present as either  $\text{MoCl}_3$  or  $\text{MoCl}_4$  [17, 18]. This lends further weight to the conclusion that a portion of

chlorine detected at the surface is associated with molybdenum species.

It has been proposed by Vukasovich and Farr [3] that the inhibiting effect of  $\text{MoO}_4^{2-}$  on the active dissolution of stainless steel is due to the formation of insoluble lower valent molybdenum oxide. In addition, Wanklyn [19] has shown that the inhibition of corrosion by Mo(VI) involves a reduction reaction. Devasenapathi and Raja [20] claim that, during stress corrosion cracking, a further mechanism of corrosion inhibition by molybdate species may be due to its ability to react with chloride according to



Thus, reducing the concentration of chloride at crack sites and reducing the susceptibility of stainless steel to corrosion.

From high resolution XPS data, obtained during these studies, it has been demonstrated that molybdenum is in a high oxidation state in uncorroded coatings on zinc electrodeposited steel panels. Through exposure to salt fog these molybdenum species are reduced to Mo(III) or Mo(IV), and from the decrease in chlorine concentration (Table 4) and the binding energies of molybdenum (Figure 8) it would appear that these species exist at the surface as chlorides. It is felt that the 'dry river bed' morphology [14] of these coatings may allow aggressive anions access to the underlying metal during exposure to corrosive environments allowing zinc oxidation to proceed. It is evident from EIS data that the presence of the conversion coating activates the metal surface during the initial stages of corrosion (Table 2, Fig. 6). This may be due to the additional cathodic process of molybdenum reduction, causing the acceleration of anodic zinc dissolution. This may explain the rapid build-up of white rust on molybdate passivated panels observed during these studies. However, observations during salt fog exposure show that the corrosion product deposit on a molybdate passivated surface, at a given time, was less severe than that present on unpassivated zinc (Table 3). This may be due to the presence of corrosion inhibiting molybdenum species at the surface during the initial stages of corrosion. The loss of molybdenum from these surfaces within 24 h of salt fog exposure (Table 4) indicates that, under the conditions studied here, molybdate coatings are unable to form the insoluble molybdenum oxides proposed by Vukasovich and Farr [3]. Instead, it appears that the species formed as a result of molybdenum reduction are soluble. Therefore, it seems that for these substrates molybdenum species may react with chloride, as described by Devasenapathi and Raja [20].

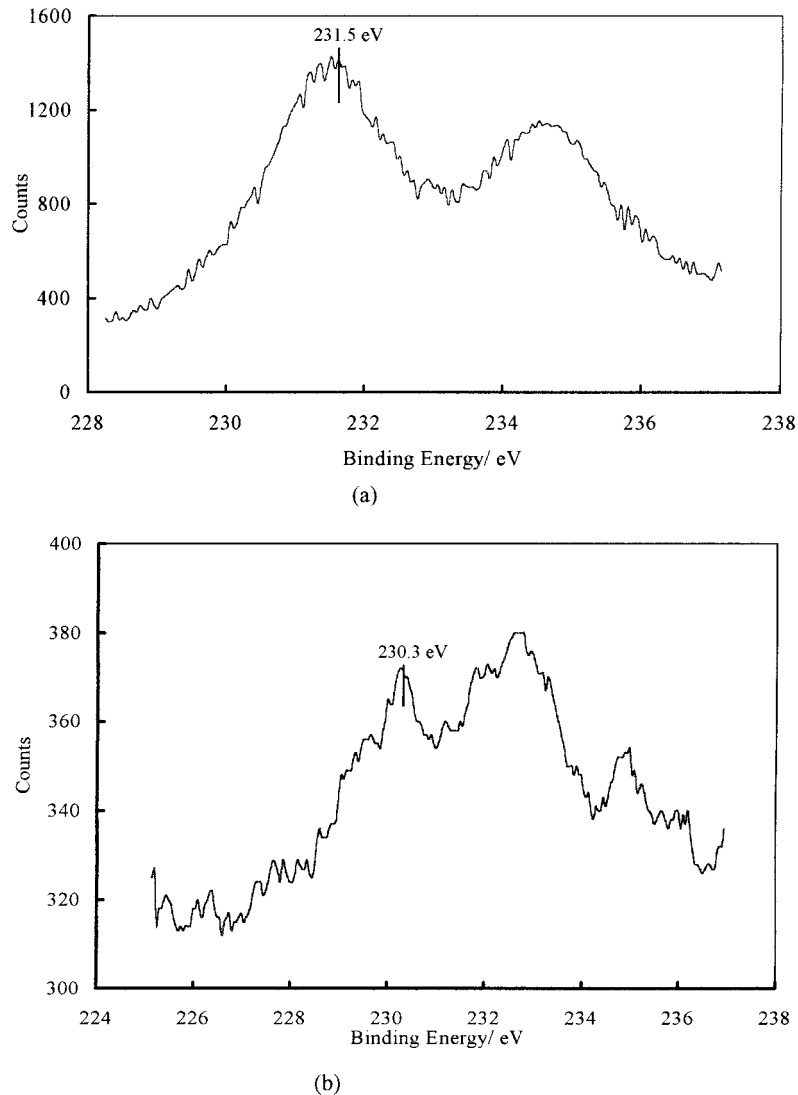


Fig. 8. XPS peaks for Mo 3d from zinc electrodeposited mild steel with a molybdate conversion coating (a) before and (b) after exposure to salt fog for 3 h. (Peaks referenced to C 1S at 285.0 eV).

The corrosion resistance of chromate conversion coatings on zinc has been ascribed to the formation of a mixed oxide containing both zinc and chromium oxide [11, 12]. In addition it is proposed that a reservoir of free Cr(VI) is present. Cr(III) species act as a barrier to corrosion, while damaged areas of the film can 'self-repair' through the reduction of Cr(VI) resulting in passivation. In the case of simple molybdate coatings on zinc electrodeposited substrates it would appear that exposure to corrosive environments causes the reduction of Mo(VI) or Mo(V) species to the, +IV or +III oxidation state. Instead of forming insoluble oxides, which could passivate the substrate surface, it would appear that the species formed are soluble and are quickly lost from the

metal surface. In addition, these coatings are cracked in nature and do not appear to possess a 'self repair' mechanism, perhaps due to the weak oxidizing nature of molybdenum in comparison with chromium. Therefore, they appear unable to prevent the build up of zinc corrosion products. The extension of time to red rust provided by molybdate conversion coatings (Table 3) may be attributable to the presence of Mo(IV) and Mo(III) species at the surface forming chloride species that reduce the concentration of aggressive ions in the corrosion layer. However, the rapid loss of these inhibiting species from the surface, due to their apparent solubility, may explain the rather poor performance of these coatings during salt fog exposure.

#### 4. Conclusions

From the data obtained during EIS analysis of these surfaces it would seem that the presence of a molybdate conversion coatings on zinc electrodeposited steel panels increases the rate of corrosion of these samples. This may be due to the ability of aggressive ions to gain access to the substrate metal through cracks in the conversion coating. The subsequent oxidation of zinc may result in the reduction of molybdenum in the conversion coating. It is felt that the slight extension of time to red rust observed during these studies (Table 3), and by other authors [9, 14], can be explained by the presence of Mo(IV) or Mo(III) species at the metal surface reacting with chloride [20]. However, the weak oxidising nature of molybdate, and the apparent solubility of the reduced molybdenum species formed, prevents corrosion resistance of the same magnitude as that provided by chromate-based coatings from being observed.

#### Acknowledgements

This work was performed with the support of the DTI-LINK Surface Engineering project Enviropass. The authors gratefully acknowledge the help of Dr I Mathieson for XPS analysis and Wm. Cannings Ltd. for the supply of materials.

#### References

1. M.S. Vukasovich, *Mater. Perform.* **29** (1990) 48.
2. M.S. Vukasovich and J.P.G. Farr, *Mater. Perform.* **25** (1986) 9.
3. M.S. Vukasovich and J.P.G. Farr, *Polyhedron* **5** (1986) 551.
4. G.D. Wilcox, D.R. Gabe and M.E. Warwick, *Corros. Rev.* **6**(4) (1986) 27.
5. G.D. Wilcox and D.R. Gabe, *Metal Finish.* (Sept. 1988) 71.
6. G.D. Wilcox, D.R. Gabe and M.E. Warwick, *Corros. Sci.* **28**(6) (1988) 577.
7. H.J. Kim and Y.K. Song, Proc. SurFin '96; Cleveland OH, June (1996), p. 123.
8. J.L. Fang, J.K. Wang, T.Q. Liu and Y. Wu, *Plat. Surf. Finish.* **82**(6) (1995) 77.
9. P.T. Tang, G. Bech-Nielsen and P. Møller, *Plat. Surf. Finish.* **81**(11) (1994) 20.
10. P.J. Anderson and M.E. Hocking, *J. Appl. Electrochem.* **8** (1958) 352.
11. E.E. Abd El Aal, A. Abd El Aal and S.M. Abd El Haleem, *Anti-Corros. Methods & Mater.* **41** (1994) 4.
12. R.H. Abu Zahra and A.M. Shams El Din, *Corros. Sci.* **5** (1965) 517.
13. H. Keping and F. Jingli, *Trans Inst. Met. Finish.* **74** (1996) 36.
14. J.A. Wharton, G.D. Wilcox and K.R. Baldwin, *Trans Inst. Met. Finish.* **74** (1996) 210.
15. B.A. Boukamp, 'Equivalent Circuit Users Manual', 2nd (revised) edn (1989).
16. T.E. Graedel, *J. Electrochem. Soc.* **136**(4) (1989) 193C.
17. D. Briggs and M.P. Seah, 'Practical Surface Analysis, Vol.1: Auger and Photoelectron Spectroscopy' (J. Wiley & Sons, New York, 1983).
18. C.D. Wagner, W.M. Riggs, L.E. Davis, J.F. Moulder and G.E. Muilenberg (Eds), 'Handbook of X-Ray Photoelectron Spectroscopy', (Perkin-Elmer Corporation, 1979).
19. J.N. Wanklyn, *Corros. Sci.* **21** (1981) 211.
20. A. Devasenapathi and V.S. Raja, *Corrosion* **52**(4) (1996) 243.